International Academic Institute for Science and Technology

International Academic Journal of Science and Engineering
Vol.11, No.1, 2024, pp.195-212.

ISSN 2454-3896

International Academic Journal of Science and Engineering

www.iaiest.com

Computational Codes for Fast Neutrons and Gamma Ray Interactions Coefficients in Different Materials

Zaid M. Nuri [a], Asmaa A. Aziz [b], Sabah M. Aman Allah [c]

Department of Physics, College of Education for Pure Sciences, Tikrit University, Tikrit, Iraq.
E-mail: zaidmznu96@gmail.com
[b] Department of Physics, College of Education for Pure Sciences, Tikrit University, Tikrit, Iraq.
E-mail: asmaa.jamal@tu.edu.iq
[c] Department of Physics, College of Education for Pure Sciences, Kirkuk University, Kirkuk, Iraq.
E-mail: hassany-2016@uokirkuk.edu.iq

Abstract

In this research, many materials used as shields against ionizing radiation (neutrons and gamma rays) were studied. Seven glass systems, compounds, and five polymeric compounds were used to test their effectiveness in attenuating fast neutrons. These compounds are (S1-S7) as shown in Table 1, and polymeric compounds as shown in Table 3. Many attenuation coefficients for these compounds were calculated through the use of a computer program called (SAZ), written in the Python programming language, which is used to calculate several basic parameters based on certain semi-empirical equations. The results showed that the sample (S7) and C_9H_9O is the best glass system compound and polymeric compound for neutron attenuation, because they have the largest value of Σ_R. Also, several Eco-friendly metallic compounds (as shown in Table 2) were used to test them in shielding against gamma rays. The mass attenuation coefficient was calculated through the NIST-XCOM program for a range of energies starting from 59.53 keV up to 1 GeV. These compounds differed in their ability to attenuate gamma rays, as the results showed that the best studied compound against gamma rays was the PbS compound because it contains the Lead element, which has the largest atomic number. This research analyzed shielding materials against fast neutrons and gamma rays using computational methods and a semi-empirical approach. Out of the seven borate glass systems and the five polymer compounds that were analyzed for fast neutron attenuation, the S7 borate and the C_9H_9O polymer were determined to be the most effective attenuation materials. In the previous study, the attenuation parameters of ΣR, HVL, TVL, and mean free path were calculated using a Python-based application called the SAZ code. As for the gamma rays, the study eventually concluded that environmentally friendly compounds like $FeCO_3$, $CaCO_3$, PbS, and $BaSO_4$ could be examined using NIST-XCOM. Of the four forementioned environmentally friendly compounds, PbS outperformed the rest due to its higher atomic number (82) and density (7.6 g/cm³). This study encourages the use of computational modeling to locate safe, effective, and sustainable shielding materials for medical or industrial purposes, or ideally in the field of nuclear applications.

Keywords: Atomic Effective Number, Attenuation Neutrons, Gamma, Molecular, Atomic, Electronic Cross Section, Half, Tenth Layer, Linear Attenuation Coefficients, NIST-XCOM, SAZ Program.

DOI:10.71086/IAJSE/V11I1/IAJSE1123
Received: 18 March 2024/Revised: 10 April 2024/Accepted: 25 April 2024/Published: 30 April 2024

Introduction

The use of nuclear technology is increasing in various fields such as medicine, particle physics, etc. There are many indirect ionizing rays, such as neutrons and gamma rays, and they have harmful effects on humans and their environment [1-3]. The susceptibility of radiation shields can be determined by reducing the intensity of the rays incident on them [4]. To choose the appropriate shielding material, you must know the type of radiation and its energy [1-3]. The best shields against neutrons are those with a small atomic number, especially those that contain hydrogen in their composition, such as plastic and water, and elements that absorb neutrons [5]. Shields against gamma rays are different than shields against neutrons, as materials with large atomic numbers are used as shields against gamma rays [1-3] [6-7]. Many studies and research have studied the attenuation parameters of neutrons and gamma rays using different methods and materials, as in [8].

Research into radiation shielding has become increasingly relevant with the emergence of new areas in nuclear medicine, industrial radiography, and power generation. When selecting an appropriate shielding material, the researcher has to reach a balance between attenuation efficiency, material availability, cost, and environmental safety. Computational methods, especially in the form of semi-empirical equations and simulation codes, allow for an efficient way for a researcher to predict shielding effectiveness before ultimately validating an experimental design. In this sense, the creation of codes to analyze neutron attenuation coefficients and gamma ray attenuation coefficients provides a straightforward mechanism of comparison across material classes. The purpose of this research is to generate greater predictive accuracy by comparing values given by calculations performed using Python with values obtained from the NIST-XCOM.

Literature Review

Prior studies have analyzed the shielding effectiveness of many materials: effective shielding materials range from traditional lead-based compounds to wild eco-friendly alternatives as in the research conducted by Elmahroug et al. (2013) about fast neutron removal cross sections for polymers and borate glasses, Alım (2020) looking at new alloys, and most recently researchers are also now discovering new compounds that have low environmental impact like $BaSO_4$ and $CaCO_3$ that provides effective shielding. Hubbell (1999) and Hubbell & Seltzer (1995) made some very important databases of photon interaction coefficients, which were extremely useful for most current shielding methods. Similar studies have been conducted in the past, but the use of computational models in material selections for neutron and gamma attenuation is extremely useful to studies like Makuch et al. (2019).

Recent studies also discussed working together computational methods with experimental measures to improve shielding effectiveness. Abdel-Rahman and Podgorsak (2010) detailed how to work through photon interactions to be able to accurately model energy transfer and deposition. Demir and Turşucu (2012) expanded on this idea by studying vitamins as a low-Z shielding option, showing that unusual materials could constitute unique uses. Al-Jaff (2013) and Allah et al. (2014) looked at steel and metallic elements and highlighted the role that atomic number and material density play in gamma attenuation. The studies emphasize that researchers seem to be leaning toward using a theoretical code, such as NIST-XCOM or a self-developed standalone program, and then verifying through experimental methods. Using a theoretical model to verify an experimental method can save a considerable amount of laboratory expenses while showing ways to use passive shielding material, which is less of a burden on the environment.

Calculations

Neutron Interactions with Matter

Neutron shielding is a complex process, due to the very wide range of neutron energies to which the shield is exposed. One of the most important of these interactions:

1. Elastic scattering: A neutron collides with the nucleus and bounces back from it like two billiard balls colliding. The neutron loses a very small portion - negligible - of its initial energy, which in turn is transferred to the nucleus as kinetic energy.
2. Inelastic scattering: Some of the neutron energy is transferred to the scattered nucleus, causing it to be excited. The nucleus usually emits gamma rays (γ) to stabilize. It is an important process when it occurs between neutrons and heavy nuclei.

3. Neutron capture: The nucleus captures neutrons to become agitated and return to stability by emitting a particle or photon of γ-rays, which is a determining factor in shielding design. Therefore, a material with a large atomic number is mixed to absorb the resulting γ-rays.
4. A neutron incident on the nucleus can cause it to fission after being absorbed, resulting in two or three additional neutrons. These additional neutrons are called fast fission neutrons.

Effective Removal Cross Section of Neutrons Σ_R $(\mathbf{cm^{-1}})$

The interaction of neutrons with materials is described by the concept of the total microscopic cross section (σ_t), which represents the probability of a neutron interacting with the atoms of the shield material, and is defined as the sum of the microscopic cross sections of scattering (σ_s) and absorption (σ_a), respectively, which is given by the relationship:

$$\sigma_t = \sigma_s + \sigma_a \ \ldots\ldots\ldots\ldots\ (1)$$

Neutron attenuation effect in matter depends on the microscopic cross-section and the number of nuclei per unit volume. These two parameters are related to the total macroscopic cross section, symbolized by Σ_t and given by:

$$\Sigma_t = \frac{\rho N_A \sigma_t}{A} \ldots\ldots\ldots\ldots (2)$$

The fast neutron removal cross section Σ_R describes the probability that the fast neutron that undergoes the first reaction is removed from the set of non-collision penetrating neutrons. Shielding materials used against neutrons are chemical compounds or mixtures, and the macroscopic removal cross-section of these materials is calculated from the microscopic removal cross-section values of their constituent elements, which can be calculated from the equation:

$$\Sigma_R = \sum_i \rho_i \left(\frac{\Sigma_R}{\rho}\right)_i \ldots\ldots\ldots\ldots . (3)$$

Where ρ_i represents the partial density measured in $\left(\frac{g}{cm^3}\right)$, and $\left(\frac{\Sigma_R}{\rho}\right)_i$ represents the mass cross-section of the removal of the (i^{th}) specific element and measured in $\left(\frac{cm^2}{g}\right)$ [28]. To calculate $\left(\frac{\Sigma_R}{\rho}\right)_i$, there are many semi-empirical relationships used for this purpose, which depend on the atomic and mass number, expressed as semi-empirical equations. One of these is the James Wood equation:

$$\frac{\Sigma_R}{\rho} = \frac{0.206}{A^{\frac{1}{3}} \cdot Z^{0.294}} \ldots\ldots\ldots (4)$$

Whereas A and Z are the mass and atomic numbers, respectively. $\frac{\Sigma_R}{\rho}$ can also be calculated from the Zoller empirical equations, which are written in the form:

$$\frac{\Sigma_R}{\rho} = \frac{0.190}{Z^{0.743}} \quad \text{when } Z \leq 8 \ \ldots\ldots . (5)$$

$$\frac{\Sigma_R}{\rho} = \frac{0.125}{Z^{0.565}} \quad \text{when } Z > 8 \ \ldots\ldots . (6)$$

The mean free path (λ), which represents the average distance that the neutron travels inside the attenuating material without interacting with it, can be measured, and it can be given by:

$$\lambda\ (\text{cm}) = \frac{1}{\Sigma_R} \ldots\ldots\ldots\ldots . (7)$$

A half-value layer (HVL) is defined as the required thickness of the attenuating material at which the intensity of the neutron rays incident on the material decreases to half its original intensity, and is calculated from the law:

$$\text{HVL(cm)} = \frac{\ln(2)}{\Sigma_R} \ldots\ldots\ldots\ldots\ldots (8)$$

A tenth value layer (TVL) represents the thickness of the material required to reduce the intensity of the neutron rays to one-tenth of their original intensity, and it can be calculated from the relation:

$$\text{TVL(cm)} = \frac{\ln(10)}{\Sigma_R} \ldots\ldots\ldots\ldots\ldots (9)$$

Table 1: Shows the Studied Samples, their Densities, Concentrations, and Thicknesses

Compounds	Samples	Concentration of PbO%	$\rho\left(\frac{g}{cm^3}\right)$	Thickness (cm)
5PbO-45BaO-50B_2O_3	S1	5	4.138	0.523
10PbO-40BaO-50B_2O_3	S2	10	4.46	0.633
15PbO-35BaO-50B_2O_3	S3	15	4.602	0.752
20PbO-30BaO-50B_2O_3	S4	20	4.744	0.834
25PbO-25BaO-50B_2O_3	S5	25	4.886	0.912
30PbO-20BaO-50B_2O_3	S6	30	5.028	1.254
35PbO-15BaO-50B_2O_3	S7	35	5.17	1.321

Equations (3-9) were used to calculate neutron attenuation parameters using the SAZ program, which is programmed using the Python programming language version 3-10-11.

The attenuation parameters were also calculated for glass borates, which are characterized by high chemical resistance and good thermal stability. It is also characterized by a low density and melting point, and with different concentrations of the PbO compound, where its concentration increases each time successfully by 5% over the previous concentration, for seven cases. In addition to the results obtained, Table 1 shows the selected samples, their symbol, concentration, density, and thickness.

Polymers are the most suitable materials as an equivalent to the tissues of human organs, as the properties of radiation interaction in human organs are studied. Polymers have different properties: light weight, flexibility, high durability, resistance to combustion, in addition to their good physical stability over a wide range of temperatures and their reasonable cost. These polymers were chosen because they contain the element hydrogen, which is a good attenuator of neutrons. It's shown in Table 4.

Gamma Ray Interaction with Matter

When gamma rays fall on materials, several interactions can occur, including:

1. Photoelectric effect: It is a process in which a photon knocks one of the electrons orbiting around an atom out of its orbit. The free electrons produced in this way are called photoelectrons, and this happens at low energies.
2. Compton scattering: It is the scattering of a photon by a free electron, and the photon transfers its energy to the electron to change the direction of its movement and energy. It is assumed that the electrons are free and do not interact with each other. The macroscopic Compton scattering cross section is determined by the electron density, and it happens at intermediate energies.
3. Pair production: A process in which a photon gives up all its energy to the surrounding vacuum, producing a pair of particles (an electron and a positron). For pair production to occur, the photon must have an initial energy greater than the mass of the electron and positron combined, $\left(1.022\,\frac{MeV}{c^2}\right)$, and it happens in the nuclear field..
4. Triple production: This process requires a threshold energy for a gamma ray photon equal to $4mc^2 = 2.044\,MeV$ and sufficient momentum to take place. This interaction takes place through the fall of a gamma ray photon on the orbiting electron to snatch it, and the gamma ray photon turns into an electron and a positron. This process results in three particles: a pair of electrons and positrons, and it happens in the atomic field.

The Mass Attenuation Coefficient $\mu_m\left(\frac{cm^2}{g}\right)$ of Gamma Ray

It's defined as a measure of the probability of the interaction that occurs between the incident photon and the target, measured in units $\left(\frac{cm^2}{\quad}\right)$/g. It is given by:

$$\mu_t = \frac{\mu}{\rho} \dots\dots\dots\dots (10)$$

Whereas $\mu(cm^{-1})$ and $\rho\left(\frac{g}{cm^3}\right)$ are the linear attenuation coefficient and the material density, respectively. For compounds and mixtures, the mass attenuation coefficient can be calculated by[1]:

$$\mu_t = \sum_i w_i(\mu_t)_i \dots\dots\dots\dots\dots (11)$$

Whereas $w_i = \frac{n_i A_i}{\sum_i n_i A_i}$ represents the weight fraction of the basic elements composing the compound or mixture, and n_i, A_i represent the number of atoms and the atomic weight, respectively, of the i^{th} specific element. Some attenuation coefficients for gamma rays, such as the total molecular cross-section $\sigma_{t,m}$, can be calculated by :

$$\sigma_{t,m} = \mu_t \frac{M}{N_A} \dots\dots\dots\dots (12)$$

Where M represents the molecular weight, and N_A represents Avogadro's number. The total atomic cross-section $\sigma_{t,a}$ can be calculated by:

$$\sigma_{t,a} = \frac{\sigma_{t,m}}{\sum_i n_i} \dots\dots\dots. (13)$$

The total electronic cross section $\sigma_{t,e}$ is calculated through the following relation:

$$\sigma_{t,e} = \frac{1}{N_A} \sum_i f_i \frac{A_i}{Z_i} (\mu_t)_i \ \dots\dots\dots. (14)$$

Whereas $f_i = \frac{n_i}{\sum_i n_i}$ represents the fractional abundance of element atoms in the compound, and Z_i represents the atomic number of the specific element. The effective atomic number Z_{eff} is calculated, which is defined as the ratio between the total atomic cross section and the total electronic cross section, and is given by:

$$Z_{eff} = \frac{\sigma_{t,a}}{\sigma_{t,e}} \dots\dots\dots.. (15)$$

The electronic density N_e describes the number of interacting electrons per unit mass of the target substance, and it can be calculated from the equation [48]:

$$N_e = \frac{\mu_t}{\sigma_{t,e}} = \frac{N_A Z_{eff}}{M} \sum_i n_i = \frac{N_A Z_{eff}}{\langle A \rangle} \dots\dots\dots\dots\dots (16)$$

Whereas $\langle A \rangle = \frac{M}{\sum_i n_i}$. To calculate the mean free path for gamma rays, the half and tenth value layers, the relationships (8,9,10) mentioned in the research can be used, respectively, within the NIST-XCOM program relationship.

Table 2: The Compounds Used in Studying Gamma Ray Attenuation, with their Densities

Composites	$\rho\left(\frac{g}{cm^3}\right)$
$FeCO_3$	3.94
$CaCO_3$	2.71
PbS	7.6
$BaSO_4$	2.96

A number of Eco-friendly compounds shown in table (2) were used in studying the attenuation of gamma rays, and a number of factors can be determined by selecting a shielding material against gamma rays, including: High atomic number, especially to get rid of heat in the inner layers of the shield, the high density of the material, which attenuates the rays more, the amount of radiation attenuation determined by the shielding material, Ease of removing heat resulting from reactions from them, thickness of the shielding material, as thickness is one of the basic factors in the shielding process, the material has good resistance to radiation damage caused by radiation exposure, The low cost of obtaining it, due to its availability in the earth's crust, Shielding materials must have high structural strength, to provide both mechanical and radiation protection, It's better for the shielding materials to be environmentally friendly, It's do not cause harm to the environment during and after their use as shielding materials, when disposed of, or when recycled .

Results and Discussion

The SAZ program (written in Python version 3.10.11) was used to calculate the neutron attenuation parameters.

Neutrons Attenuations (Glass Borate System PbO-BaO-B_2O_3) - Calculations

Figure 1 shows the effective removal cross-section Σ_R and the concentration of PbO. It was found that its highest value was for sample S7, and the minimum value was for sample S1. We notice that Σ_R increases almost directly with increasing concentration of PbO content in the samples within the range (5-35) mol%. This can be attributed to the gradual increase in the sample density when the concentration of PbO increases. This means that the neutron

attenuation properties of these samples improve with the increase in the concentration of PbO content. The current is in good agreement with the results.

Figure 2) shows the mean free path λ and PbO concentration. We notice that λ decreases gradually and almost inversely with increasing PbO concentration. Also, we note that its largest value was for the sample S1, and the results show a good agreement.

Table 3: Shows the Values of the Seven Attenuation Parameters Calculated Using the SAZ Code and Comparing them with the Results

Samples	$\Sigma_R(cm^{-1})$			λ(cm)			HVL (cm)			TVL (cm)		
	James	Zoller	[39]	James	Zoller	[39]	James	Zoller	[39]	James	Zoller	[39]
S1	0.13761	0.13216	0.1322	7.2669	7.5667	7.5636	5.0370	5.2448	5.2427	16.7327	17.4229	17.4159
S2	0.14134	0.13579	0.1358	7.0751	7.3645	7.3616	4.9041	5.1047	5.1026	16.291	16.9574	16.9506
S3	0.14502	0.13937	0.1394	6.8955	7.1752	7.1723	4.7796	4.9734	4.9715	15.8774	16.5214	16.5149
S4	0.14865	0.14291	0.1430	6.7271	6.9976	6.9949	4.6628	4.8503	4.8485	15.4897	16.1125	16.1063
S5	0.15223	0.1464	0.1465	6.5689	6.8307	6.8281	4.5532	4.7347	4.7329	15.1254	15.7282	15.7222
S6	0.15576	0.1498	0.1499	6.4200	6.6736	6.6711	4.4500	4.6258	4.6241	14.7827	15.3665	15.3608
S7	0.15924	0.15324	0.1533	6.2798	6.5255	6.5231	4.3528	4.5231	4.5215	14.4597	15.0256	15.0200

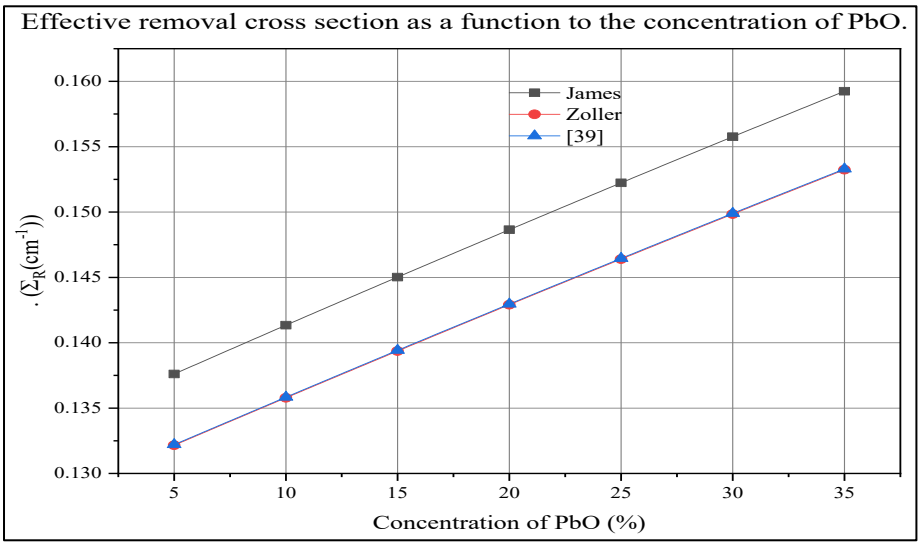


Fig. 1: Shows Effective Removal Cross Section and Concentration

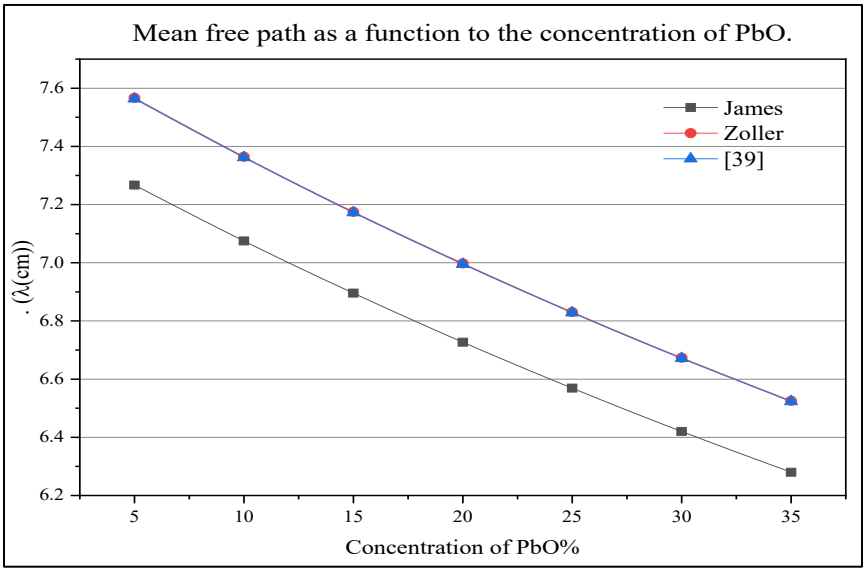


Fig. 2: Shows the Mean Free Path and Concentration

Figures (3 and 4) show the half, tenth value layer (HVL, TVL) and concentration of PbO. The (HVL&TVL) gradually decreases with an increase in the concentration of PbO in the samples. Increasing the concentration leads to an increase in the density and thickness of the samples, and this leads to an increase in the amount of attenuation of the fast neutrons. The largest (HVL&TVL) values were within sample S1, while the lowest and best values were in sample S7; the results closely matched, meaning that it's possible to use these materials as shielding materials against neutrons.

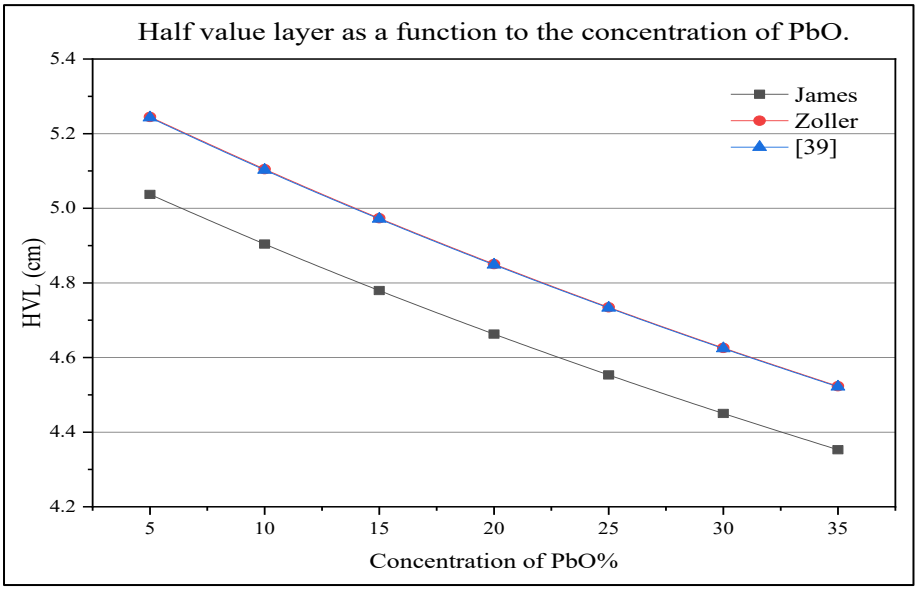


Fig. 3: Shows Half Value Layer and Concentration

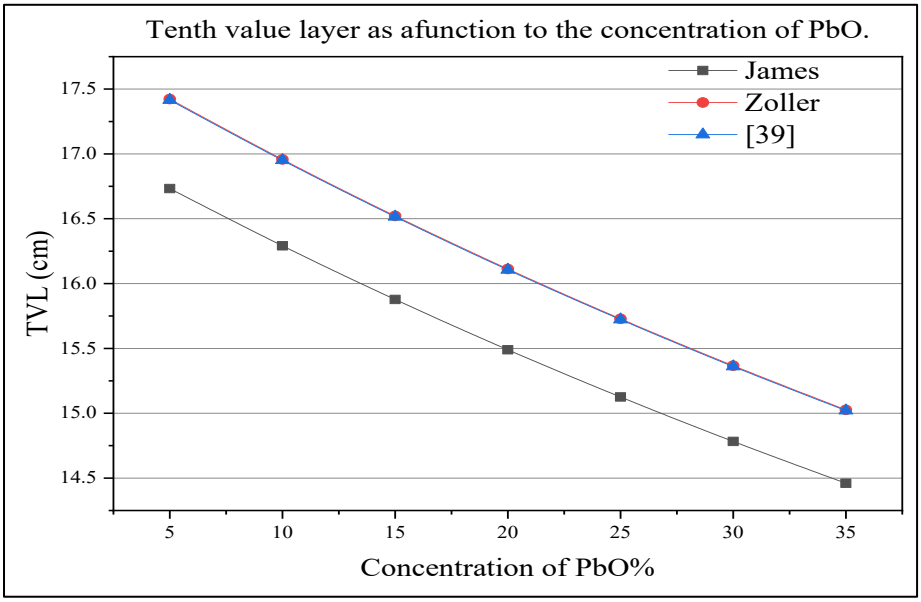


Fig. 4: Shows the Tenth Value Layer and Concentration

Neutrons Attenuation by Polymers - Calculations

Figure (5) shows the effective removal cross-section Σ_R, and it was found that the compound C_9H_9O has the biggest value, the reason for this is the presence of a large percentage of the hydrogen element in the compound, as the neutron interacts with the hydrogen nucleus in an elastic collision, as that Σ_R depends on the chemical content of the compound and its density [8]. The sample $C_5H_8O_2$ had the lowest value of Σ_R, due to its chemical content of oxygen

and carbon, and its relatively small mass density compared to the sample with the highest value of Σ_R [8]. Neutron attenuation also depends on the number of nuclei of the compound and its macroscopic cross section Σ_t.

Table 4: Shows the Values of the Parameters that Were Theoretically Calculated Using the SAZ Code

Polymer	$\rho\left(\frac{g}{cm^3}\right)$	$\frac{\Sigma_R}{\rho}\left(\frac{cm^2}{g}\right)$		$\Sigma_R(cm^{-1})$		λ(cm)		HVL(cm)		TVL(cm)	
		James	Zoller	James	Zoller	James	Zoller	James	Zoller	James	Zoller
C_3H_6	0.90	0.2591	0.2402	0.0676	0.0633	14.7947	15.8098	10.2549	10.9585	34.0659	36.4034
$C_5H_8O_2$	0.95	0.3035	0.2807	0.0595	0.0554	16.8042	18.0368	11.6478	12.5021	38.6932	41.5312
C_8H_8	1.06	0.2591	0.2402	0.0689	0.0647	14.5209	15.4627	10.0651	10.7179	33.4357	35.6042
C_2H_3Cl	1.30	0.2865	0.2654	0.0597	0.0556	16.7515	17.9780	11.6112	12.4614	38.5717	41.3959
C_9H_9O	1.45	0.3035	0.2807	0.0906	0.0849	11.0359	11.7789	7.6495	8.1645	25.4111	27.1219

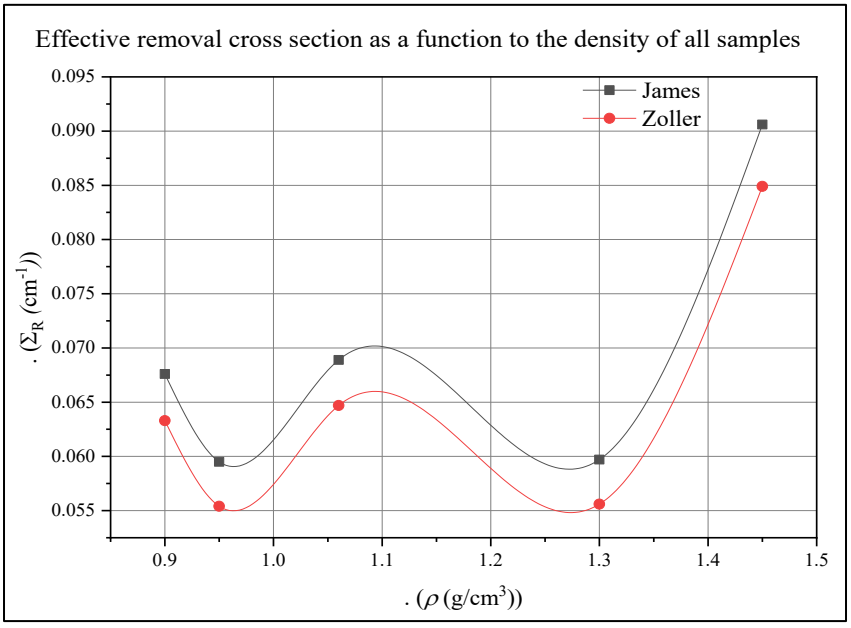


Fig. 5: Shows Effective Removal Cross Section and Density for Fast Neutron

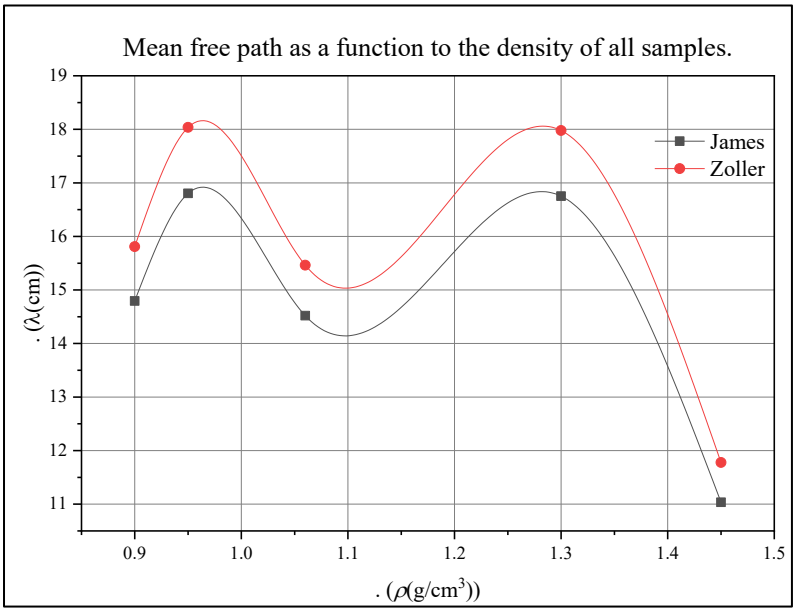


Fig. 6: Shows Mean Free Path and Density for Fast Neutron

Figure 6 shows the mean free path λ. The lowest value was for the sample C_9H_9O. This is expected due to the inverse relationship between Σ_R and λ. The reason for this small amount is due to the small rate of collisions with the nucleus of the hydrogen atom to which the neutron is exposed to transform into a thermal neutron. The nucleus absorbed it, and the highest value obtained was for the sample $C_5H_8O_2$, due to the increase in the number of oxygen atoms. Figures (7 and 8) show the half, tenth value layer (HVL, TVL). The highest values were for sample $C_5H_8O_2$, and the lowest values were for sample C_9H_9O due to the inverse relationship between (HVL, TVL) and Σ_R. This can be explained by the chemical content of the samples that contain carbon and oxygen, which require a large collision rate with fast neutrons to be converted into thermal neutrons by elastic scattering.

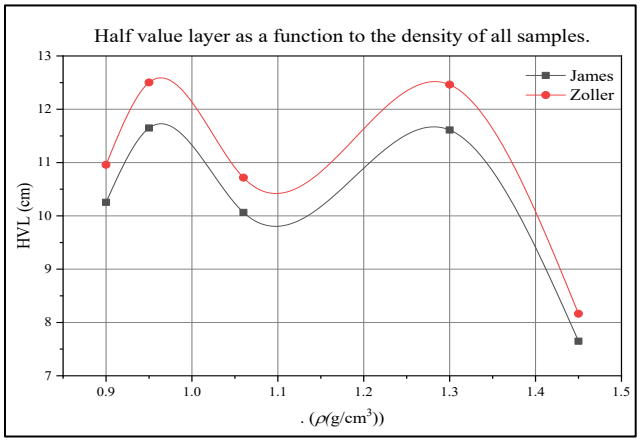


Fig. 7: Shows the Half Value Layer and Density for Fast Neutron.

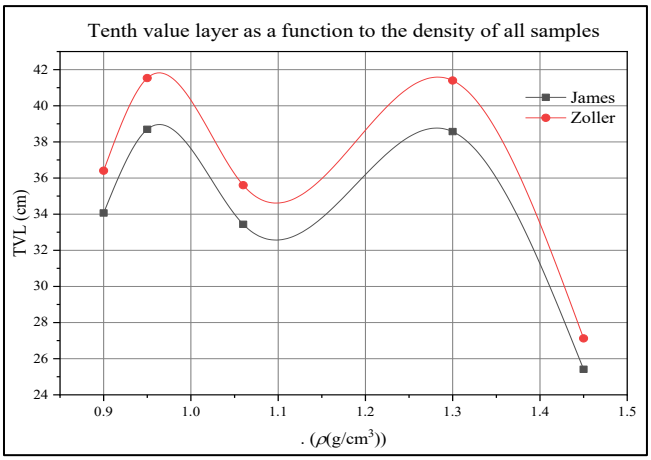


Fig. 8: Shows the Tenth Value Layer and Density for Fast Neutron

The ratio of the final energy of the neutron to its initial energy with which it is released can be determined through the relationship:

$$\frac{E_f}{E_i} = \frac{A^2 + 2A \cdot \cos\theta + 1}{(A+1)^2} \dots\dots\dots\dots (20)$$

Whereas A is the mass number, θ is the scattering angle, and when $A = 1$ – for the hydrogen element – the lost energy will be as large as possible, due to the great convergence between the mass of the neutron and the mass of the proton, and when the collision between the neutron and the nucleus is vertical ($\theta = 0$), the neutron It loses all its energy at once, and from this we conclude that elastic scattering is the most common reaction in attenuated media in which hydrogen is the most common.

Gamma Ray's Attenuation - Calculations

NIST-XCOM data was relied upon to calculate the attenuation parameters for gamma rays. Table (5) shows the results of mass attenuation coefficient μ_t for several mineral compounds shown in Table (2) by application of the XCOM code, and the results showed that μ_t decreases with increasing energy of the incident photon. The compound

$BaSO_4$ has the highest value of μ_t at the lowest energy, because the compound contains the relatively large element barium with atomic number 56, and the lowest value for the compound $CaCO_3$ at the same energy, because it contains relatively light elements, and this can be attributed to the large σ_{pe} of gamma ray attenuation, which It is proportional to $\frac{Z^{4.6}}{E^{3.5}}$, where the photoelectric phenomenon is dominant. At medium energies, Compton scattering is dominant, as σ_{cs} is proportional to $\frac{Z}{E}$ [5], and we notice that μ_t begins to increase slightly, and that is because the cross section is proportional to Z^2, where the pair production reaction is dominant. Table 6 shows linear attenuation coefficient values μ and energy. The μ decreases with increasing energy of the incident photon and then increases slightly at high energies. The highest value was for the compound PbS, and the lowest value was for the compound $CaCO_3$ at the same energy. The large value of μ for the compound PbS compared to other compounds is due to the high density of the compound, and also because it contains lead with a high atomic number, as the linear attenuation coefficient depends on the density of the material.

Table 7 shows the total molecular cross section $\sigma_{t,m}$, which is large at small photon energies and gradually decreases with increasing energy. The largest value of $\sigma_{t,m}$ is for the compound $BaSO_4$ because $\sigma_{t,m}$ is directly proportional to μ_t, due to the large σ_{pe} at the lowest energy, and the compound $CaCO_3$ is the least valuable due to its low density and containing light elements.

Table (8) shows the total atomic cross section $\sigma_{t,a}$, which is large and then gradually decreases up to energies (10-70) MeV and then begins to increase slightly with increasing energy, where the phenomenon of pair production is most influential. The largest value of $\sigma_{t,a}$ was for the compound PbS, and the discrepancy between the values of $\sigma_{t,a}$ and $\sigma_{t,m}$ appears for the compounds PbS and $BaSO_4$ due to the difference in the number of their atoms. The lowest value for $\sigma_{t,a}$ at the same energy was for the compound $CaCO_3$, due to the presence of elements with low atomic number in it.

Table 5: Mass Attenuation Coefficient Versus Photon Energy

	$\mu_t(cm^2/g)$			
Energy (MeV)	$FeCO_3$	$CaCO_3$	PbS	$BaSO_4$
0.05953	0.6904	0.3812	4.491	5.223
0.08099	0.3649	0.2426	2.066	2.338
0.12178	0.2019	0.1681	2.951	0.8381
0.24469	0.1199	0.1184	0.558	0.2065
0.35601	0.1	0.1013	0.2624	0.1279
0.364	0.09899	0.1006	0.2521	0.125
0.66166	0.0754	0.0775	0.1058	0.0775
0.7789	0.06987	0.07189	0.0887	0.06999
0.96413	0.06302	0.06492	0.07233	0.06169
1.17323	0.0571	0.05888	0.06135	0.05508
1.25	0.05529	0.05703	0.05851	0.05321
1.3325	0.05352	0.05518	0.05601	0.05142
1.40801	0.05203	0.05364	0.05411	0.04996
2.75	0.03748	0.03834	0.04226	0.03768
7.12	0.02668	0.0263	0.04305	0.03241
10	0.02512	0.02374	0.04653	0.03307
20	0.02451	0.022	0.05713	0.03717
30	0.02531	0.02219	0.06431	0.04057
40	0.02619	0.02268	0.06953	0.0432
50	0.027	0.0232	0.07351	0.04528
60	0.02771	0.02368	0.07666	0.04695
70	0.02833	0.02413	0.07923	0.04835
80	0.02889	0.02453	0.08137	0.04953
90	0.02938	0.02489	0.08319	0.05055
100	0.02981	0.02522	0.08475	0.05144
200	0.03246	0.02731	0.09342	0.05652
300	0.03374	0.02836	0.09725	0.05885

400	0.03451	0.029	0.09947	0.0602
500	0.03503	0.02945	0.1009	0.06111
600	0.03541	0.02977	0.102	0.06177
700	0.0357	0.03002	0.1027	0.06226
800	0.03592	0.03021	0.1034	0.06264
900	0.03611	0.03037	0.1039	0.06295
1000	0.03626	0.0305	0.1043	0.06321

Table 6: Linear Attenuation Coefficient Versus Photon Energy

	μ (cm^{-1})			
Energy (MeV)	$FeCO_3$	$CaCO_3$	PbS	$BaSO_4$
0.05953	2.72018	1.03305	34.1316	15.46008
0.08099	1.43771	0.65745	15.7016	6.92048
0.12178	0.79549	0.45555	22.4276	2.48078
0.24469	0.47241	0.32086	4.2408	0.61124
0.35601	0.394	0.27452	1.99424	0.37858
0.364	0.39002	0.27263	1.91596	0.37
0.66166	0.29719	0.21005	0.80408	0.22949
0.7789	0.27529	0.19482	0.67412	0.20717
0.96413	0.2483	0.17593	0.54971	0.1826
1.17323	0.22497	0.15956	0.46626	0.16304
1.25	0.21784	0.15455	0.44468	0.1575
1.3325	0.21087	0.14954	0.42568	0.1522
1.40801	0.205	0.14536	0.41124	0.14788
2.75	0.14767	0.1039	0.32118	0.11153
7.12	0.10512	0.07127	0.32718	0.09593
10	0.09897	0.06434	0.35363	0.09789
20	0.09657	0.05962	0.43419	0.11002
30	0.09972	0.06013	0.48876	0.12009
40	0.10319	0.06146	0.52843	0.12787
50	0.10638	0.06287	0.55868	0.13403
60	0.10918	0.06417	0.58262	0.13897
70	0.11162	0.06539	0.60215	0.14312
80	0.11383	0.06648	0.61841	0.14661
90	0.11576	0.06745	0.63224	0.14963
100	0.11745	0.06835	0.6441	0.15226
200	0.12789	0.07401	0.70999	0.1673
300	0.13294	0.07686	0.7391	0.1742
400	0.13597	0.07859	0.75597	0.17819
500	0.13802	0.07981	0.76684	0.18089
600	0.13952	0.08068	0.7752	0.18284
700	0.14066	0.08135	0.78052	0.18429
800	0.14152	0.08187	0.78584	0.18541
900	0.14227	0.0823	0.78964	0.18633
1000	0.14286	0.08266	0.79268	0.1871

Table 7: Total Molecular Cross Section Versus Photon Energy

	$\sigma_{t-molecular}$ (barn/molecule)			
Energy (MeV)	$FeCO_3$	$CaCO_3$	PbS	$BaSO_4$
0.05953	132.8002	63.34572	1784.06	2023.118
0.08099	70.18942	40.31393	820.723	905.6192
0.12178	38.83597	27.93393	1172.291	324.6362
0.24469	23.06306	19.67506	221.6667	79.98733

0.35601	19.23525	16.83348	104.239	49.54179
0.364	19.04097	16.71715	100.1473	48.41848
0.66166	14.50915	12.88019	42.02928	30.03108
0.7789	13.43967	11.94628	35.23627	27.11047
0.96413	12.12205	10.78805	28.73325	23.89549
1.17323	10.98333	9.784354	24.37142	21.33512
1.25	10.63517	9.476932	23.24323	20.61078
1.3325	10.2947	9.169509	22.2501	19.91743
1.40801	10.0081	8.9136	21.49532	19.3519
2.75	7.209371	6.37113	16.78788	14.59527
7.12	5.131964	4.370389	17.10171	12.55394
10	4.831894	3.944983	18.48414	12.80959
20	4.714559	3.655839	22.69502	14.39772
30	4.868441	3.687412	25.54729	15.7147
40	5.037712	3.768838	27.62095	16.73343
50	5.193517	3.855248	29.20201	17.53911
60	5.330087	3.935012	30.45335	18.18598
70	5.449346	4.009791	31.47429	18.72827
80	5.557063	4.07626	32.32441	19.18534
90	5.651316	4.136083	33.04741	19.58043
100	5.734027	4.190921	33.66712	19.92517
200	6.243762	4.538226	37.1113	21.8929
300	6.489973	4.712709	38.63278	22.79542
400	6.638084	4.81906	39.51468	23.31834
500	6.738107	4.893839	40.08275	23.67083
600	6.811201	4.947015	40.51972	23.92648
700	6.866984	4.988558	40.7978	24.11628
800	6.909301	5.020132	41.07588	24.26347
900	6.945848	5.046719	41.2745	24.38355
1000	6.974701	5.068322	41.4334	24.48426

Table (9) shows the total electronic cross section $\sigma_{t,e}$, as it is large at small photon energies, where the phenomenon of photoelectric interaction is most likely, then it decreases to a certain extent, and then it increases slightly. The largest value of $\sigma_{t,e}$ at the lowest energy is for the compound $BaSO_4$, and the lowest value for $\sigma_{t,e}$ at the same energy is for the compound $CaCO_3$, and this can be explained by the big difference in Z present in the two compounds.

The effective atomic number Z_{eff}, we note that its value is constant for all the energies studied, as it is equal to (11.1712,10.0087,48.7478,17.1846) for the compounds ($FeCO_3$, $CaCO_3$, PbS, $BaSO_4$) respectively, and its value varies depending on the chemical composition of the compound. The highest value is for PbS, because it contains the Lead element with a large Z, and the lowest value is for $CaCO_3$, because it contains relatively light elements.

Since the electronic density N_{ele} is related to Z_{eff}, its relationship with energy is also constant. The values of N_{ele} are equal to (2.904, 3.012, 2.4543, 2.6619)$\times 10^{23}\left({}^{e}/_{g}\right)$ for compounds ($FeCO_3$, $CaCO_3$, PbS, $BaSO_4$) respectively, and the highest value is for $CaCO_3$, because it is inversely proportional to the electronic cross section. The minimum value is for PbS, which has a large molar mass compared to the compound $CaCO_3$.

Table (10) shows the mean free path λ, it is small and increases rapidly with the increase in photon energy until it reaches its highest value at approximately 30 MeV for the compound $CaCO_3$, then it begins to decrease slowly, that is, when it appears pair production is the most common, while the lowest value of λ is for PbS at the same energy.

This is because PbS is a high-density compound with a relatively large effective atomic number compared to $CaCO_3$, which has a low density and an effective atomic number.

Tables (11 & 12) show the half, tenth value layer (HVL, TVL), which is inversely proportional to μ, as they have a small value at low energies, then increase with increasing energy. Their highest values were for the compound $CaCO_3$, and their lowest values were for the compound PbS, which means high attenuation efficiency for this compound. The reason for the difference in density of the two compounds is their containment of elements with significantly different atomic numbers.

Table 8: Total Atomic Cross Section Versus Photon Energy

	$\sigma_{t-atomic}$ (barn/atom)			
Energy (MeV)	$FeCO_3$	$CaCO_3$	PbS	$BaSO_4$
0.05953	26.56	12.6691	892.0298	337.186
0.08099	14.0379	8.0628	410.3615	150.937
0.12178	7.7672	5.5868	586.146	54.106
0.24469	4.6126	3.935	110.8334	13.3312
0.35601	3.8471	3.3667	52.1195	8.257
0.364	3.8082	3.3434	50.0736	8.0697
0.66166	2.9018	2.576	21.0146	5.0052
0.7789	2.6879	2.3893	17.6181	4.5184
0.96413	2.4244	2.1576	14.3666	3.9826
1.17323	2.1967	1.9569	12.1857	3.5559
1.25	2.127	1.8954	11.6216	3.4351
1.3325	2.0589	1.8339	11.1251	3.3196
1.40801	2.0016	1.7827	10.7477	3.2253
2.75	1.4419	1.2742	8.3939	2.4325
7.12	1.0264	0.8741	8.5509	2.0923
10	0.9664	0.789	9.2421	2.1349
20	0.9429	0.7312	11.3475	2.3996
30	0.9737	0.7375	12.7736	2.6191
40	1.0075	0.7538	13.8105	2.7889
50	1.0387	0.7711	14.601	2.9232
60	1.066	0.787	15.2267	3.031
70	1.0899	0.802	15.7372	3.1214
80	1.1114	0.8153	16.1622	3.1976
90	1.1303	0.8272	16.5237	3.2634
100	1.1468	0.8382	16.8336	3.3209
200	1.2488	0.9076	18.5557	3.6488
300	1.298	0.9425	19.3164	3.7992
400	1.3276	0.9638	19.7573	3.8864
500	1.3476	0.9788	20.0414	3.9451
600	1.3622	0.9894	20.2599	3.9877
700	1.3734	0.9977	20.3989	4.0194
800	1.3819	1.004	20.5379	4.0439
900	1.3892	1.0093	20.6373	4.0639
1000	1.3949	1.0137	20.7167	4.0807

Table 9: Total Electronic Cross Section Versus Photon Energy

	$\sigma_{t-electroic}$ (barn/electron)			
Energy (MeV)	$FeCO_3$	$CaCO_3$	PbS	$BaSO_4$
0.05953	1.2566	0.8056	8.4181	8.7832
0.08099	0.6953	0.5582	12.0241	3.1485
0.12178	0.4129	0.3932	2.2736	0.7758

0.24469	0.3444	0.3364	1.0692	0.4805
0.35601	0.3409	0.3341	1.0272	0.4696
0.364	0.2598	0.2574	0.4311	0.2913
0.66166	0.2406	0.2387	0.3614	0.2629
0.7789	0.217	0.2156	0.2947	0.2318
0.96413	0.1966	0.1955	0.25	0.2069
1.17323	0.1904	0.1894	0.2384	0.1999
1.25	0.1843	0.1832	0.2282	0.1932
1.3325	0.1792	0.1781	0.2205	0.1877
1.40801	0.1291	0.1273	0.1722	0.1416
2.75	0.0919	0.0873	0.1754	0.1218
7.12	0.0865	0.0788	0.1896	0.1242
10	0.0844	0.0731	0.2328	0.1396
20	0.0872	0.0737	0.262	0.1524
30	0.0902	0.0753	0.2833	0.1623
40	0.093	0.077	0.2995	0.1701
50	0.0954	0.0786	0.3124	0.1764
60	0.0976	0.0801	0.3228	0.1816
70	0.0995	0.0815	0.3315	0.1861
80	0.1012	0.0827	0.339	0.1899
90	0.1027	0.0837	0.3453	0.1932
100	0.1118	0.0907	0.3806	0.2123
200	0.1162	0.0942	0.3963	0.2211
300	0.1188	0.0963	0.4053	0.2262
400	0.1206	0.0978	0.4111	0.2296
500	0.1219	0.0989	0.4156	0.2321
600	0.1229	0.0997	0.4185	0.2339
700	0.1237	0.1003	0.4213	0.2353
800	0.1244	0.1008	0.4233	0.2365
900	0.1249	0.1013	0.425	0.2375
1000	0.1249	0.1013	0.425	0.2375

Table 10: Mean Free Path Versus Photon Energy

	λ(cm)			
Energy (MeV)	$FeCO_3$	$CaCO_3$	PbS	$BaSO_4$
0.05953	0.367623	0.968005	0.029298	0.064683
0.08099	0.695552	1.521037	0.063688	0.144499
0.12178	1.257093	2.195144	0.044588	0.4031
0.24469	2.116823	3.116585	0.235805	1.636019

0.35601	2.538071	3.642682	0.501444	2.641422
0.364	2.563967	3.668029	0.521932	2.702703
0.66166	3.364803	4.760724	1.243657	4.357511
0.7789	3.632562	5.132893	1.483415	4.826944
0.96413	4.027406	5.683976	1.819148	5.476379
1.17323	4.444958	6.267046	2.144726	6.133585
1.25	4.59047	6.470344	2.248828	6.349142
1.3325	4.742285	6.687272	2.349205	6.570164
1.40801	4.878092	6.879263	2.431694	6.762166
2.75	6.771801	9.624509	3.113558	8.965972
7.12	9.51301	14.03056	3.056422	10.42388
10	10.10379	15.54354	2.82783	10.21584
20	10.35525	16.7729	2.30315	9.088992
30	10.02794	16.62928	2.046011	8.327282
40	9.690993	16.27	1.892405	7.82032
50	9.400263	15.90533	1.789946	7.461083
60	9.159405	15.58293	1.716396	7.195694
70	8.958952	15.29232	1.660721	6.987339
80	8.785293	15.04296	1.617045	6.820873
90	8.638771	14.82538	1.581668	6.683241
100	8.51416	14.63139	1.552554	6.56761
200	7.819073	13.51167	1.408467	5.977315
300	7.522439	13.01141	1.352997	5.74066
400	7.354596	12.72427	1.3228	5.611924
500	7.245421	12.52984	1.304053	5.528356
600	7.167668	12.39515	1.28999	5.469287
700	7.109443	12.29193	1.281197	5.426242
800	7.065899	12.21462	1.272524	5.393324
900	7.028721	12.15027	1.2664	5.366765
1000	6.999644	12.09848	1.261543	5.34469

Table 11: Half Value Layer Versus Photon Energy

	HVL(cm)			
Energy (MeV)	$FeCO_3$	$CaCO_3$	PbS	$BaSO_4$
0.05953	0.2548	0.671	0.0203	0.0448
0.08099	0.4821	1.0543	0.0441	0.1002
0.12178	0.8714	1.5216	0.0309	0.2794
0.24469	1.4673	2.1603	0.1634	1.1340
0.35601	1.7593	2.5249	0.3476	1.8309

0.364	1.7772	2.5425	0.3616	1.8734
0.66166	2.3323	3.2999	0.8620	3.0204
0.7789	2.5179	3.5579	1.0282	3.3458
0.96413	2.7916	3.9398	1.2609	3.7959
1.17323	3.0810	4.344	1.4866	4.2515
1.25	3.1819	4.4849	1.5588	4.4009
1.3325	3.2871	4.6353	1.6283	4.5541
1.40801	3.3812	4.7683	1.6855	4.6872
2.75	4.6939	6.6712	2.1582	6.2147
7.12	6.5939	9.7252	2.1186	7.2253
10	7.0034	10.774	1.9601	7.0811
20	7.1777	11.626	1.5964	6.3000
30	6.9508	11.527	1.4182	5.7720
40	6.7173	11.278	1.3117	5.4206
50	6.5158	11.025	1.2407	5.1716
60	6.3488	10.801	1.1897	4.9877
70	6.2099	10.599	1.1511	4.8433
80	6.0895	10.427	1.1209	4.7279
90	5.9879	10.276	1.0963	4.6325
100	5.9016	10.142	1.0761	4.5523
200	5.4198	9.3656	0.9763	4.1432
300	5.2142	9.0188	0.9378	3.9791
400	5.0978	8.8198	0.9169	3.8899
500	5.0221	8.6850	0.9039	3.832
600	4.9682	8.5917	0.8942	3.7910
700	4.9279	8.5201	0.8881	3.7612
800	4.8977	8.4665	0.8820	3.7384
900	4.8719	8.4219	0.8778	3.7200
1000	4.8518	8.3860	0.8744	3.7047

Table 12: Tenth Value Layer Versus Photon Energy

	TVL(cm)			
Energy (MeV)	$FeCO_3$	$CaCO_3$	PbS	$BaSO_4$
0.05953	0.846484	2.228915	0.067462	0.148937
0.08099	1.601569	3.502318	0.146647	0.33272
0.12178	2.894564	5.054506	0.102667	0.928171
0.24469	4.874166	7.176203	0.54296	3.767072
0.35601	5.844125	8.387585	1.154618	6.082098
0.364	5.903753	8.445948	1.201792	6.223203

0.66166	7.747746	10.96197	2.863627	10.03354
0.7789	8.364283	11.81892	3.41569	11.11445
0.96413	9.273444	13.08784	4.188742	12.60983
1.17323	10.23489	14.43041	4.938414	14.1231
1.25	10.56995	14.89852	5.178119	14.61944
1.3325	10.91952	15.39801	5.409243	15.12836
1.40801	11.23222	15.84009	5.599182	15.57046
2.75	15.59265	22.16125	7.169231	20.64491
7.12	21.90451	32.30655	7.037671	24.00186
10	23.26483	35.79033	6.51132	23.52284
20	23.84384	38.62102	5.303198	20.92818
30	23.09018	38.29033	4.711114	19.17428
40	22.31434	37.46307	4.357424	18.00695
50	21.64491	36.62338	4.121504	17.17978
60	21.09031	35.88101	3.952149	16.5687
70	20.62875	35.21187	3.823952	16.08894
80	20.22888	34.63768	3.723384	15.70564
90	19.89151	34.1367	3.641925	15.38873
100	19.60458	33.69002	3.574888	15.12248
200	18.00408	31.11177	3.243114	13.76328
300	17.32106	29.95989	3.11539	13.21836
400	16.93458	29.2987	3.04586	12.92193
500	16.6832	28.85102	3.002693	12.72951
600	16.50416	28.54089	2.970311	12.5935
700	16.3701	28.30321	2.950065	12.49438
800	16.26983	28.1252	2.930094	12.41859
900	16.18423	27.97703	2.915993	12.35743
1000	16.11728	27.85778	2.90481	12.3066

Conclusions

In this research, neutron attenuation parameters were studied for several polymers and glass systems, to measure the effectiveness of these materials in shielding against fast neutrons through the use of specific empirical equations, the mass removal cross-section $\left(\frac{\Sigma_R}{\rho}\right)$, the effective removal cross-section of Σ_R, the mean free path, and half, tenth value layers were calculated. It was also shown that sample S7 in the glass borate system has the best attenuation parameters, as it was found to have the best values for Σ_R, which, according to the experimental equations, are equal to $0.15924\ \mathrm{cm}^{-1}$, $0.15324\ \mathrm{cm}^{-1}$, and $0.1533\ \mathrm{cm}^{-1}$, respectively. This means that it is the best sample to use as an attenuation shield against neutrons. From present calculations of Σ_R for various compounds, it's clear that the compound C_9H_9O has the largest value among the samples, which is equal to $0.0906\ \mathrm{cm}^{-1}$ and $0.0849\ \mathrm{cm}^{-1}$, respectively, which means that it is more suitable. In the design of shields against neutrons. The current study showed that the compound PbS has the best attenuation coefficients against gamma rays because it contains the Lead element, which has a high density and atomic number, followed by the compound BaSO4. The results

reaffirm the importance of computer codes for materials screening as an expedited material screening process for radiation shielding. The comparative analysis with NIST-XCOM and validating that the results are consistent between both codes further establishes the reliability of the SAZ code and its practicality of application, not only in research but also in industrial design as well. The research shows that green compounds can potentially provide adequate shielding without the reliance on heavy metals, which can reflect the sustainability goals. Future works, similar to the current study, should consider the experimental justification of these results, develop polymer-high-Z composites or hybrid composites, and also implement machine learning to predict shield properties. Integration of these variables will ultimately provide more efficient, affordable, or green shielding methods.

References

Hubbell, J.H. (1999). Review of photon interaction cross-section data in the medical and biological context. *Physics in Medicine & Biology*, *44*(1), R1.

Hubbell, J.H., & Seltzer, S.M. (1995). *Tables of X-ray mass attenuation coefficients and mass energy-absorption coefficients 1 keV to 20 MeV for elements Z= 1 to 92 and 48 additional substances of dosimetric interest* (No. PB-95-220539/XAB; NISTIR-5632). National Inst. of Standards and Technology-PL, Gaithersburg, MD (United States). Ionizing Radiation Div.

Hubbell, J.H. (1982). Photon mass attenuation and energy-absorption coefficients. *The International Journal of Applied Radiation and Isotopes*, *33*(11), 1269-1290.

Abdel-Rahman, W., & Podgorsak, E.B. (2010). Energy transfer and energy absorption in photon interactions with matter revisited: A step-by-step illustrated approach. *Radiation Physics and Chemistry*, *79*(5), 552-566.

Chilton, A.B., Shultis, J.K., & Faw, R.E. (1984). Principles of radiation shielding.

Alım, B. (2020). A comprehensive study on radiation shielding characteristics of Tin-Silver, Manganin-R, Hastelloy-B, Hastelloy-X, and Dilver-P alloys. *Applied Physics A*, *126*(4).

Demir, D., & Turşucu, A. (2012). Studies on mass attenuation coefficient, mass energy absorption coefficient, and kerma of some vitamins. *Annals of Nuclear Energy*, *48*, 17-20.

Elmahroug, Y., Tellili, B., & Souga, C. (2013). Calculation of fast neutron removal cross-sections for different shielding materials. *International Journal of Physics and Research (IJPR)*, *3*(2), 7-16.

Al-Jaff, S. (2013). Investigation of the effective atomic number, electron density, half value layer, and mean free path of steel types304and 347 in the energy range 40–130 *keV. J. Nat. Sci. Res, 5,* 2225-2921.

Allah, S.M.A., Abdala, R., Aziz, A.A., & Aboead, A.M. (2014). Calculating the Effective atomic number, electron density, half-value layer, and mean free path of Iron, Copper, and Silver. *Diyala Journal for Pure Science*, *10*(3), 32-43.